Ab initio GW electron-electron interaction effects in quantum transport

Pierre Darancet,[1,2] Andrea Ferretti,[3] Didier Mayou,[1] and Valerio Olevano[1]
[1]*Institut Néel, UPR 2940 CNRS, BP 166, 38042 Grenoble, France and European Theoretical Spectroscopy Facility (ETSF)*
[2]*Université Joseph Fourier, BP 53, 38042 Grenoble, France*
[3]*Dipartimento di Fisica, Università di Modena e Reggio Emilia, and INFM-CNR-S3, National Center on nanoStructures and bioSystems at Surfaces, 41100 Modena, Italy and European Theoretical Spectroscopy Facility (ETSF)*
(Received 14 November 2006; published 7 February 2007)

We present an *ab initio* approach to electronic transport in nanoscale systems which includes electronic correlations through the *GW* approximation. With respect to Landauer approaches based on density-functional theory (DFT), we introduce a physical quasiparticle electronic structure into a nonequilibrium Green's function theory framework. We use an equilibrium non-self-consistent G^0W^0 self-energy considering both full non-Hermiticity and dynamical effects. The method is applied to a real system, a gold monoatomic chain. With respect to DFT results, the conductance profile is modified and reduced by the introduction of diffusion and loss-of-coherence effects. The linear response conductance characteristics appear to be in agreement with experimental results.

DOI: 10.1103/PhysRevB.75.075102 PACS number(s): 72.10.Di, 71.10.−w, 72.15.Nj, 73.63.−b

Electronics at the nanoscale—namely, *nanoelectronics*—represents the next years' technological challenge. It is boosted not only by the need for shorter integration scales, but also by the expectation that unusual quantum effects[1] are going to be observed due to quantum phenomena effects. Beside the experimental efforts to synthesize nanoelectronic devices, quantum transport theory[2] has the formidable task of understanding and modeling the mechanisms behind these phenomena and to predict them from a first-principles approach.

In the last years, a combination of *ab initio* density-functional theory (DFT) calculations together with the description of transport properties in a Landauer-Büttiker (LB) framework[2] has demonstrated its ability to describe small-bias coherent transport in nanojunctions.[3–5] These approaches were successful in accounting for the contact resistance and conductance degrading mechanisms induced by impurities, defects, and noncommensurability patterns in the conductor region. The major objections raised to such method are that (i) the Kohn-Sham (KS) electronic structure is in principle unphysical, to be considered only as an approximation to the quasiparticle (QP) electronic structure; (ii) noncoherent and dissipative effects due to electron-phonon (*e*-ph) and electron-electron (*e*-*e*) scattering can be taken into account only approximatively in the LB formalism; (iii) nonlinear response and far-from-equilibrium finite-bias transport are not accessible, since DFT cannot be applied to open systems and is not a nonequilibrium theory (although recent works[6] have demonstrated that *time-dependent* DFT can tackle the problem).

Nonequilibrium Green's function (NEGF) theory[7,8] is in principle a correct approach to address the above objections. The critical point within this theory is the choice of good approximations to the self-energy Σ^r and coherently to the scattering functions $\Sigma^{<,>}$. This ensures that both the renormalization of the QP energies and the electron diffusion mechanisms due, e.g., to *e*-ph or *e*-*e* interactions will be properly taken into account. The first works studying the role of the *e*-ph coupling[9,10] and of short-range *e*-*e* correlations[11,12] or the renormalization of the QP energies[13] have recently appeared in the literature or, we are aware, are going to appear.[14] The role of correlations, apart from being central in explaining, e.g., Coulomb blockade and Kondo effects, could also be crucial in bridging the gap between experimentally observed and LB-predicted conductances, which in some cases are orders of magnitude off.[6,12,15]

In this work, we introduce electronic correlations in the calculation of transport by an *ab initio* approach based on Hedin's *GW* approximation[16,17] (GWA) in the framework of NEGF. In our scheme, the *GW* self-energy is built at equilibrium and the Green's function is calculated by direct solution of the Dyson equation. For the lead/conductor/lead geometry, the *GW* self-energy is summed to the lead's self-energies; the electronic conductance is calculated through the Meir-Wingreen formula,[19] a NEGF Landauer-like expression derived for interacting conductors. We apply this scheme to a realistic system, a gold monoatomic unidimensional chain,[20] and we study the effects induced on transport properties by the different components of the *GW* self-energy, the Hermitian and the non-Hermitian parts, and the dynamical dependence. Our results show that the conductance profile is considerably modified by the real part of the *GW* correction. The imaginary part introduces a suppression of the conductance, which is negligible close to the Fermi energy, but that increases with the energy. Finally, the full dynamical dependence of the *GW* self-energy introduces further structures far from the Fermi energy, which have to be ascribed to satellite excitations of the system. The *GW* smooth drop on the conductance characteristics as a function of the bias at very low voltage compares favorably with the trend experimentally measured in gold nanowires.[20]

With respect to the Hartree-Fock (HF) approach, which already renormalizes the energies for the *e*-*e* classical repulsion and exchange, the GWA introduces the important contribution due to correlations and to *e*-*e* scattering diffusion mechanisms responsible for loss of coherence in transport. Indeed, by direct inspection of the diagrammatic representation of the two-particle Green's function G_2 (see Fig. 1 and Refs. 7 and 18), one can see that the G_2^{HF} describes an

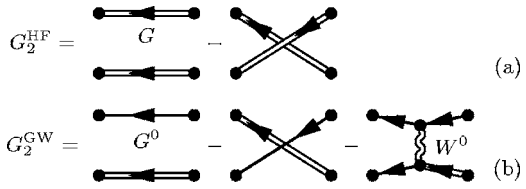

FIG. 1. Two-particle Green's function in the self-consistent Hartree-Fock (a) and in the non-self-consistent G^0W^0 approximation (b). Thin line: non-self-consistent G^0. Double line: self-consistent G. Wiggly line: RPA non-self-consistent W^0.

uncorrelated propagation and that collisional terms are missing. This implies that the HF scattering functions $\Sigma^<$ and $\Sigma^>$ are exactly zero. On the other hand, even a non-self-consistent G^0W^0 approximation introduces a collisional term [the last diagram in Fig. 1(b)] which gives rise to nonzero $\Sigma^{<,>}$ and in turn to *e-e* scattering mechanisms and incoherent, dissipative effects in transport. As is shown by the corresponding G_2 Feynman diagram, the G^0W^0 approximation is not a conserving approximation in the Baym-Kadanoff sense,[7] leading to, e.g., nonconservation of the number of particles. However, the relative deviation from the exact density brought by the G^0W^0 approximation has been evaluated by Schindlmayr *et al.*[18] to be only of the order of 0.05% for the range of metallic densities ($r_s^{\mathrm{Au}}=3.01$) of interest here.

Our starting point is a standard DFT-LDA calculation based on plane waves (PW's) and norm-conserving pseudopotentials for an infinite monoatomic chain of gold atoms using periodic boundary conditions.[21] The KS electronic structure is calculated both at the relaxed atomic distance (4.72 bohrs) and in a *stretched* geometry (5.32 bohrs), so as to simulate the experimental situation described in Ref. 20 [conductance measures of a gold monoatomic chain pulled up from a gold surface by an scanning tunneling microscope (STM) tip] and also the calculations reported in Ref. 9. From the DFT KS eigenfunctions, we obtain an orthonormal set of *maximally localized* Wannier functions (MLWF's),[22] which are used as a basis set in the calculation of quantum transport. The following step is a converged[23] *GW* plane-wave calculation of both the QP energies and the self-energy matrix elements for the six bands around the Fermi energy, corresponding to the gold *sd* manifold. The self-energy in the G^0W^0 approximation at equilibrium is given by

$$\Sigma_{GW}(\omega) = \frac{i}{2\pi}\int_{-\infty}^{\infty} d\omega' e^{-i\omega' 0^+} G^0(\omega-\omega')W^0(\omega'), \quad (1)$$

where G^0 is the Green's function built on the noninteracting KS electronic structure and W^0 is the dynamically screened interaction given by the random phase approximation (RPA) polarizability $P^{\mathrm{RPA}}=-iG^0G^0$. Since for transport we need a fine-grid fully dynamical dependence of the self-energy, we calculate the frequency integral of Eq. (1) in three different ways: (i) by approximating the dynamical dependence of $W(\omega')$ through a *plasmon-pole* (PP) model;[17] (ii) by a *contour deformation* (CD) method,[24] which consists in a deformation of the real axis contour such that the self-energy can be calculated as an integral along the imaginary axis minus a contribution arising from the residual of the contour-included poles of G; (iii) by an *analytic continuation* (AC) method,[25]—i.e., calculating the integral and also the self-energy on the imaginary axis and then performing an analytical continuation to the real axis. In the last step we carried out the quantum transport calculation using a modified version of the WANT code.[3,11] We first projected the *GW* self-energy, as well as the noninteracting Hamiltonian H^0, on the Wannier functions basis set (nondiagonal self-energy elements in the Bloch basis were neglected). We study the bulk conductance and also partition the system into three regions: the right (R) and left (L) leads—two semi-infinite gold monoatomic chains—and a central (C) region, constituted by a single gold atom. This has the purpose of clarifying the role of both intraconductor and conductor-lead correlations. We calculate the retarded Green's function in the space spanned by the MLWF set by inverting the Dyson equation—i.e.,

$$G^r(\omega) = [\omega - H^0 - \Sigma^r(\omega)]^{-1}, \quad (2)$$

where H^0 is the KS Hamiltonian once the exchange-correlation contribution is subtracted, $H^0=H_{\mathrm{KS}}-V_{xc}$. For the tripartitioned geometry, the total retarded self-energy

$$\Sigma^r = \Sigma_L^r + \Sigma_R^r + \Sigma_{GW}^r \quad (3)$$

is the sum of the correlation *GW* and lead self-energies. The conductance is finally calculated using the following formula:

$$C(\epsilon) = \frac{2e^2}{h}\mathrm{tr}[G^a\Gamma_R G^r \Gamma_L(\Gamma_L+\Gamma_R)^{-1}\Gamma], \quad (4)$$

first given by Meir and Wingreen[19] and recently rederived under more general conditions.[11] Here $\Gamma=\Gamma_L+\Gamma_R+\Gamma_{GW}$, not to be confused with the vertex function, is the *total decay rate* (the sum of the electron in- and out-scattering functions), due to both the presence of the R and L leads and the effect of the *e-e* interaction,

$$\Gamma = i(\Sigma^r - \Sigma^a) = i(\Sigma^> - \Sigma^<). \quad (5)$$

With respect to the Landauer formula, Eq. (4) presents a factor $(\Gamma_L+\Gamma_R)^{-1}\Gamma$ which reduces to 1 in the uncorrelated case. Equation (4) represents an *effective* (including correlation effects) transmission probability of an electron injected at energy ϵ through the conductor.

In Figs. 2(a) and 2(b) we compare the DFT-LDA (Kohn-Sham) and the *GW* (quasiparticle) electronic structure for the relaxed geometry. The dots represent the DFT-LDA levels from the PW calculation. We verified that the diagonalization on the MLWF basis (solid lines) closely reproduces the PW results. Squares, triangles, and diamonds represent the *GW* electronic structures calculated using the PP model, CD method, and AC method, respectively. Little difference among the *GW* methods is found. The *GW* corrections globally lower the *d*-like states with respect to the Fermi level and also reduce the *s*-like bandwidth (this effect is less evident in the stretched chain where the bandwidth shrinks about 3 eV already at the DFT level).

In Fig. 2, we compare the real and imaginary parts of the self-energy (d) and the spectral function $A=i(G^r-G^a)$ (c) for a point close to the Fermi level. We remark that the AC

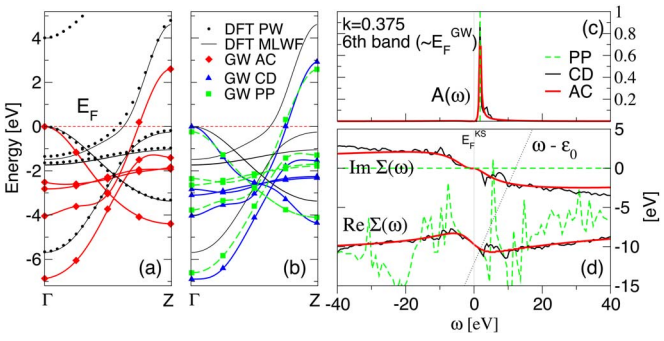

FIG. 2. (Color online) (a) and (b) DFT-LDA Kohn-Sham vs *GW* electronic structure: Black dots: DFT-LDA on PW basis. Lines: DFT-LDA on MLWF. Squares, triangles, and diamonds refer to *GW* calculations from the PP model, CD method, and AC method, respectively. The Fermi energy is set to zero. (c) Spectral function and (d) real and imaginary parts of the *GW* self-energy: dashed, thin, and thick lines are from the PP model, CD method, and AC method, respectively. The dotted curve is the straight line $\omega-\epsilon^K S+\langle V_{xc}\rangle$ whose intersections with the real part of the self-energy give the peaks of the spectral function. The 0 is set to the Kohn-Sham Fermi energy.

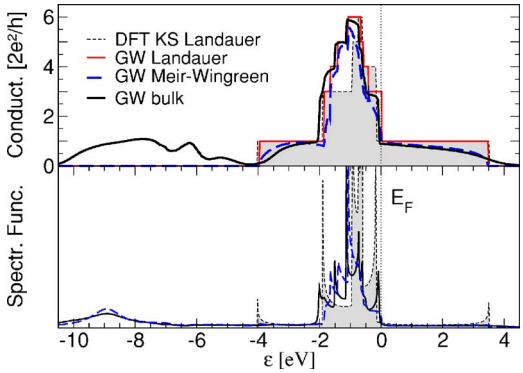

FIG. 3. (Color online) Conductance (top) and spectral function (bottom) for the stretched atomic configuration. The Fermi level is set to zero. Thin dashed line: Landauer result using a DFT KS structure. Thin solid line: Landauer using only a real-part *GW* renormalization of the energies. Thick dashed line: Meir-Wingreen result using a *GW* real-part renormalization in the leads and a full (Hermitian+anti-Hermitian) dynamical *GW* self-energy in the conductor. Thick solid line: *GW* bulk conductance with full dynamical self-energy.

method appears to smooth the richer-in-structure CD spectrum. Although computationally cheaper, the AC method should be considered less accurate than the CD method, especially in the imaginary part. However, the frequency dependence as well as the shape and the position of the main structures (both QP and satellites peaks) are essentially caught by both methods. Therefore, we use the AC approach in the following.

In Fig. 3 we show the conductance and the spectral function of the gold chain for the stretched geometry, obtained using different methods: The thin dashed line is calculated using the Landauer formula and the DFT KS electronic structure. The conductance at the Fermi level for the stretched chain appears to be 1 (in units of $2e^2/h$), and it is of *s*-like character. This is true also for the relaxed structure (not shown), although in that case the Fermi level is at the limit of the onset of the *d*-like states. The thin solid line is obtained from the Landauer formula evaluated using the *GW* real-part-only QP energies. *GW* corrections are considered both in the conductor and in the leads. Otherwise, a ficticious contact resistance, unphysical for a homogeneous system, would appear. At this first level, the net effect is a renormalization of KS into QP energies, the true energies to introduce and remove an electron from the system. Therefore, the GWA affects the conductance profile by modifying the position of the conductance steps, especially in the *d*-like region. In the relaxed geometry, the GWA also narrows the *s*-like conductance channel.

The thick dashed line in Fig. 3 represents the result obtained in the tripartitioned geometry by using the Meir-Wingreen formula and introducing a full non-Hermitian and dynamical *GW* self-energy in the conductor. Static real-part-only QP energies are included in the leads. This introduces loss of coherence only in the conductor while leaving the leads ballistic. At the same time it *limits* the introduction of ficticious contact resistances; i.e., the QP levels are aligned in the leads and the conductor. The difference of this curve with respect to the thin solid line genuinely represents the effect of *e*-*e* scattering mechanisms in the conductor, causing diffusion, loss of coherence, and appearance of resistance. With respect to Landauer approaches, the spectral function now appears as a collection of broadened QP peaks, whose finite width is directly associated to the inverse of the electronic lifetime of the QP state. The spectral weight, which is spread out, results in a lowering and a spill-out of the conductance step-like profile. This effect is directly related to the imaginary part of the QP energies and can be seen to increase with $\epsilon-E_F$ although not with a quadratical scaling Fermi-liquid behavior, as is normally observed in *GW* results for three-dimensional systems. Finally, we calculate the fully correlated bulk *GW* conductance by taking into account a non-Hermitian and dynamical *GW* self-energy everywhere in the system, conductor, and leads (thick solid line). With respect to the previous case, even residual contact resistances (due to the fact that the conductor and lead spectral peaks were differently shaped, with finite and infinitesimal widths, respectively) are completely removed and the conductance increases almost overall. Only around −3 eV do we see a slight drop, which is due to the specific $(\Gamma_L+\Gamma_R)^{-1}\Gamma$ factor in Eq. (4). Moreover, new structures appear in the conductance at the lowest energies. By inspecting the spectral function, we can attribute them to the presence of satellites of electronic origin—i.e., plasmons or shake-ups—of the main QP peaks. Since the *e*-*e* interaction is an elastic scattering mechanism, these satellites are necessary to balance the losses which occur at energies close to the Fermi level and are therefore important for transport. The *e*-*e* scattering acts in a way to redistribute the conductance channels to different energies, rather than globally destroy conductance as in the *e*-ph scattering, where momentum and current is lost to ionic degrees of freedom.

Taking the *GW* bulk result, we have integrated the conductance curve such to obtain the voltage characteristics of the correlated system. We compare with the experimental results of Ref. 20 and the *e*-ph result of Ref. 9, calculated at

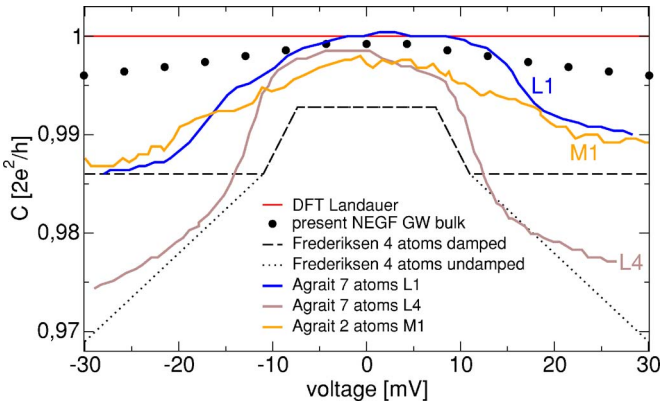

FIG. 4. (Color online) Differential conductance vs applied bias. Thin solid line: DFT Landauer result. Dots: present NEGF *GW* bulk result for the 5.35 bohr interatomic distance; dashed-dotted line: *e*-ph theory of Ref. 9 corresponding to four atoms, the same interatomic distance, and for the damped and undamped limits. Thick solid lines: experimental result of Ref. 20 corresponding to two and seven atoms and different chain strains.

exactly the same stretched 5.35 bohr interatomic distance. Like in that work, we assume that an equilibrium picture can still be appropriate to describe the small voltage range of ±30 mV. The *GW* result is shown in Fig. 4 (dots). The results from Ref. 9 attribute the step in the conductance, occurring at ~15 mV, to the onset of phononic processes. Instead, the continuous drop observed in our electronic correlated conductance, occurring in the first 15 mV, compares favorably with the drop observed experimentally:[20] *e-e* scattering mechanisms seem hence responsible for the conductance drops at very low bias.[26] While the quantitative agreement with the experiment on the conductance value may be somewhat fortuitous,[27] the trend in this drop is a direct consequence of the increase in the *GW* imaginary part of QP energies.

In conclusion, we have calculated the conductance of a realistic gold chain system by taking into account *e-e* correlation effects within the *GW* approximation. With respect to Landauer DFT results, the conductance profile is considerably modified. Already at the level of an equilibrium nonself-consistent *GW* approximation, the trend of the differential conductance appears to compare favorably with the trend experimentally observed for this system.

We thank L. Reining, D. Feinberg, H. Mera, M. Verstraete, Y. M. Niquet, and E. Shirley for useful discussions and remarks. Computer time has been granted by IDRIS Project No. 060932. A.F. acknowledges funding by Italian MIUR through PRIN 2004.

[1] J. Park, A. N. Pasupathy, J. I. Goldsmith, C. Chang, Y. Yaish, J. R. Petta, M. Rinkoski, J. P. Sethna, H. D. Abruna, P. L. McEuen, and D. C. Ralph, Nature (London) **417**, 722 (2002); P. Jarillo-Herrero, J. Kong, H. S. J. van der Zant, C. Dekker, L. P. Kouwenhoven, and S. De Franceschi, *ibid.* **434**, 484 (2005); Z. Yao, H. Postma, L. Balents, and C. Dekker, *ibid.* **402**, 273 (1999).

[2] S. Datta, *Electronic Transport in Mesoscopic Systems* (Cambridge University Press, New York, 1995).

[3] A. Calzolari, N. Marzari, I. Souza, and M. B. Nardelli, Phys. Rev. B **69**, 035108 (2004); see also http://www.wannier-transport.org

[4] M. Brandbyge, J.-L. Mozos, P. Ordejón, J. Taylor, and K. Stokbro, Phys. Rev. B **65**, 165401 (2002); J. J. Palacios, A. J. Pérez-Jiménez, E. Louis, E. SanFabián, and J. A. Vergés, Phys. Rev. Lett. **90**, 106801 (2003).

[5] S. Latil, S. Roche, D. Mayou, and J.-C. Charlier, Phys. Rev. Lett. **92**, 256805 (2004); F. Triozon, S. Roche, A. Rubio, and D. Mayou, Phys. Rev. B **69**, 121410(R) (2004).

[6] S. Kurth, G. Stefanucci, C.-O. Almbladh, A. Rubio, and E. K. U. Gross, Phys. Rev. B **72**, 035308 (2005); N. Sai, M. Zwolak, G. Vignale, and M. Di Ventra, Phys. Rev. Lett. **94**, 186810 (2005).

[7] L. P. Kadanoff and G. Baym, *Quantum Statistical Mechanics* (Banjamin, New York, 1962).

[8] H. Haug and A.-P. Jauho, *Quantum Kinetics in Transport and Optics of Semiconductors* (Springer, Berlin, 1996).

[9] T. Frederiksen, M. Brandbyge, N. Lorente, and A. P. Jauho, Phys. Rev. Lett. **93**, 256601 (2004).

[10] N. Sergueev, D. Roubtsov, and H. Guo, Phys. Rev. Lett. **95**, 146803 (2005).

[11] A. Ferretti, A. Calzolari, R. Di Felice, F. Manghi, M. J. Caldas, M. B. Nardelli, and E. Molinani, Phys. Rev. Lett. **94**, 116802 (2005); A. Ferretti, A. Calzolari, R. Di Felice, and F. Manghi, Phys. Rev. B **72**, 125114 (2005).

[12] P. Delaney and J. C. Greer, Phys. Rev. Lett. **93**, 036805 (2004).

[13] A. Pecchia, A. Di Carlo, A. Gagliardi, T. A. Niehaus, and T. Frauenheim, J. Comput. Electron. **4**, 79 (2005).

[14] K. S. Thygesen and A. Rubio, cond-mat/0609223 (unpublished).

[15] F. Evers, F. Weigend, and M. Koentopp, Phys. Rev. B **69**, 235411 (2004).

[16] L. Hedin, Phys. Rev. **139**, 796 (1965).

[17] M. S. Hybertsen and S. G. Louie, Phys. Rev. Lett. **55**, 1418 (1985); R. W. Godby and R. J. Needs, *ibid.* **62**, 1169 (1989).

[18] A. Schindlmayr, P. García-González, and R. W. Godby, Phys. Rev. B **64**, 235106 (2001).

[19] Equation (10) in Y. Meir and N. S. Wingreen, Phys. Rev. Lett. **68**, 2512 (1992).

[20] N. Agraït, C. Untiedt, G. Rubio-Bollinger, and S. Vieira, Phys. Rev. Lett. **88**, 216803 (2002).

[21] Gold 6*s* and 5*d* electrons are kept in valence. We adopt a cutoff of 30 Ry for wave functions and a (8, 1, 1) *k* grid.

[22] N. Marzari and D. Vanderbilt, Phys. Rev. B **56**, 12847 (1997).

[23] We used 150 and 100 states to converge W and Σ, respectively; 2503 plane waves have been used to represent the wave functions and Σ_x, while the dimension of the Σ_c and W reciprocal-space matrices was 49. Imaginary axis integrations were carried out by a Gauss quadrature using 30 nodes. In the analytical continuation, we used a Padé approximant on 12 nodes. We used a modified version of the ABINIT code.

[24] A. Fleszar and W. Hanke, Phys. Rev. B **56**, 10228 (1997).

[25] H. N. Rojas, R. W. Godby, and R. J. Needs, Phys. Rev. Lett. **74**, 1827 (1995).

[26] G.-M. Rignanese, X. Blase, and S. G. Louie, Phys. Rev. Lett. **86**, 2110 (2001).

[27] In general the *GW* approximation does not achieve such levels of accuracy.